

Plate Scattering Visualization: Images, Near Fields, Currents, and Far Field Patterns

John Shaeffer
Marietta Scientific, Inc.
376 Powder Springs St. 240A
Marietta, Georgia 30064
(770) 425-9760

Kam Hom
NASA Langley Research Center
Hampton, Virginia 23665

ABSTRACT: This paper presents a case study of a simple yet robust target for demonstration of the EM visualization process. A five lambda square plate exhibits many scattering mechanisms depending on excitation angle and polarization: specular scattering, leading and trailing edge diffraction, traveling wave, and edge wave scattering. Bistatic k space radiation images, currents maps, and near scattered / total fields are examined for each of these scattering mechanisms.

Visualization in Computational Electromagnetics: The ultimate goal of computational modeling is to predict observed phenomena. Thus, for many years, computational scattering or antenna EM modeling output consisted of a backscatter or antenna radiation pattern that was compared to experimental results. In this mode, computational modeling did little to aid the identification and understanding of the physical mechanisms responsible for observed behavior. This limitation was unfortunate. Computational EM codes should in principle be able to provide a rich insight to the scattering or radiation process if we just ask the proper questions and use the rapidly developing graphical display capabilities to illustrate the basic phenomena. Our EM visualization inspiration is similar to efforts in computational fluid dynamics. We are attempting to better understand the interaction of an EM wave or local excitation with a structure, the nature of body-body interactions, and the nature of the resultant radiation.

Visualization diagnostics for electromagnetics involve the display of body currents, near fields and radiation images. Each display tells us something different about the radiation process. Taken together, these diagnostics produce a richer understanding of complex EM phenomena.

Currents (or effective tangential magnetic or electric fields) are the fundamental quantities which produce far field radiation patterns and are often the computational goal, e.g. MOM codes. Knowledge of the current amplitude and phase distribution on a geometric structure is sufficient to compute the radiation pattern. Although a graphical display of currents indicates the spatial amplitude distribution, it does not tell *how* the currents radiate in different directions in space.

Displays of near field E and H indicate how one part of a structure interacts with another part, how the surface currents and charges begin to form the eventual far-field radiation pattern and how various surface current modes are formed such as surface and edge traveling-wave mechanisms.

Bistatic k space imaging is yet another diagnostic tool for examining the scattering/radiation process. An image is not a picture of currents, but of the far field radiation produced by the currents. Images differ from a body current distribution in that an image shows *how* the currents radiate. An image from a given angle tells us which *parts* of the current distribution are producing radiation in that direction.

Far field radiation is the phasor sum of signals from *all* radiation centers on the body that radiate in the observed direction. An image identifies each center as a separate entity. The utility of images results from the ability to separate and identify the individual radiation centers that have collectively summed to produce the net result. This enables us to understand the nature of each radiation center and to modify it in ways that might be useful.

Visualization Parameters: Bistatic k-Space images [1-3] show the current distribution regions that radiate into the direction of the observer. These images do not require a frequency sweep, as do conventional experimental images. They are obtained by from the current distribution by evaluating the far field radiation integral over down and cross range directions in k-space and then performing a Fourier transform. One, two and three-dimensional images can be computed.

Surface currents, the computational goal of MOM codes, are the source of the observed visualization parameters: images, near fields, and far-scattered fields.

Currents and near fields are complex quantities. The real and imaginary parts represent the two independent time solutions corresponding to the phase of the incident excitation, time $t = 0$ and -90 degrees of the excitation. Time harmonic animation is obtained by adding these two basis solutions. A time average root mean square (RMS) value is the value observed experimentally.

Near fields are computed from the current and charge distribution. Scattered fields are those produced directly by the currents. Total fields are the sum of the incident field with the scattered field.

Plate Geometry: The plate is square with side dimension of five wavelengths, Figure 1. The MOM code solution was obtained using MOM3D [4] and the visualization was obtained using EM ANIMATE [5]. Plane waves were used to excite the plate.

Far Field Backscatter Patterns: The traditional prediction code output for the backscatter patterns are shown in Figure 2. The elevation cut perpendicular to the plate edges, (a), shows the backscatter magnitudes for specular, end region, traveling wave and edge diffraction. The elevation cut along the plate diagonal, (b), shows the backscatter due to specular, traveling wave and end region mechanisms. The azimuth cut in the plane of the plate for horizontal polarization, (c), has edge wave and edge specular scattering mechanisms.

Visualization: Current and field contour plots have a reverse gray scale. High values are black and low values are light.

Perpendicular Excitation: The induced plate currents, Figure 3, have the nominal physical optics value of twice the incident magnetic field along with a smaller component flashing back and forth between the edges forming a standing wave component. The scattered field produced by these currents radiates broadside to the plate on each side. Plate regions appear as line sources. The total field is perpendicular to the plate (as required by the PEC boundary conditions). The time average total field shows a shadow region behind the plate where the scattered and incident fields phase subtract. In front of the plate the total field shows a standing wave pattern resulting from the interference of the incident and scattered fields. The first peak occurs at $\lambda/4$ above the plate. The resultant backscatter from these currents is the broadside-specular value of $\frac{1}{2}$. The backscatter two-dimensional bistatic k space image shows a distributed source across the plate where each portion of the current distribution is contributing to the scattered field. The distributed image magnitude has a value that depends on the effective image resolution and coherent length [1].

45° Slant Angle Excitation: At 45° incidence with E parallel to the plate edge, Figure 4, the plate currents are still physical optics like with linear phase and a leading edge line source due to edge diffraction. The scattered field shows two major phenomena. The leading edge diffraction line currents are producing a cylindrical scattered wave while the physical optics currents are producing a forward and reflected scattered field symmetric about the plate. The total field shows the shadow formed on the plate backside and an interference pattern on the upper side. The backscatter bistatic k space image shows the leading and trailing edge of the plate as the major sources of radiation. The leading edge current line source is dominant.

0° Edge On Excitation: Edge illumination with E parallel to the edge, the major plate currents are the leading edge diffraction currents and two edge wave components which reflect from the rear plate vertices, Figure 5. The scattered field now is due mostly to leading edge diffraction line currents and is a cylindrical wave centered at the leading edge. The total field shows the shadow behind the plate and the interference pattern from the incident and scattered fields. The backscatter bistatic k space image shows the leading edge diffraction line source as the dominant scattering source. Secondary scattering sources are the two edge waves reflecting from the rear plate vertices. The line source backscatter magnitude is dependent on the plate edge length, L .

Traveling Wave Excitation at 22.5°: For vertical polarization near grazing, backscatter is due to a traveling wave reflected by the rear edge, Figure 6. The angle up from grazing at which this mechanism peaks is given by $\theta = 22.5^\circ$. The traveling wave return is very similar to trailing edge diffraction for surface only a few wavelengths in size. The surface current display clearly shows the build up of the traveling wave as it builds in magnitude as it propagates aft on the plate where it reflects. The scattered field shows: 1) the surface wave on the plate; 2) the specular forward and reflected wave; and 3) the field produced by the reflected traveling wave which appears to emanate from the trailing edge. The total field shows the shadow behind the plate as well as the interference pattern between the scattered and incident fields. The backscatter bistatic k space image clearly shows the entire plate contributing to the scattered field with the

trailing edge being the peak. This is consistent with the notion that the surface current reflected wave loses energy via radiation after reflection from the back edge.

Edge Wave Excitation: When the plate is illuminated with horizontal polarization in plane the plane of the plate along the diagonal, backscatter is due to two edge waves reflected from the mid vertices, Figure 7. The current visualization clearly shows the edge currents flowing down the two illuminated edges. The scattered field in a plane along the plate diagonal shows the front tip diffraction. The total field shows the shadow and the interference pattern between scattering and incident fields. The backscatter bistatic k space image clearly shows the source as the two reflected edge waves. Note that the peak is at the mid vertices. The edge wave decays as it radiates away from the reflection point. A smaller amount of scattering is from the rear vertex due to edge waves that “turned” the first corner and are now being reflected from the back tip.

Traveling Wave Excitation Along Diagonal: For vertical polarization up 22.5° from grazing, a surface traveling wave is formed, Figure 8. Now, however, the rear reflection point is the rear vertex. The surface current visualization clearly shows the build up of the surface currents as the wave travels aft on the plate as it gains energy from the incident field. The scattered field in a plane along the plate diagonal shows the surface traveling wave on the plate. The scattered field from the rear vertex is apparently much smaller than the forward scattered energy and is not seen. The total field shows the interference pattern between the scattered and incident fields. The backscatter bistatic k space image shows the aft vertex region as the major source of backscatter. This is entirely consistent with the concept of the reflection of the surface traveling wave.

VFY218 Aircraft: A combined visualization for a non-simple scattering body is shown in Figure 9. The configuration is the VFY218 EMCC benchmark aircraft [6]. The illumination is nose on, horizontal polarization. Surface currents are displayed on the aircraft body. Scattered fields are shown in a vertical plane down the length of the vehicle. The backscatter bistatic k space image is shown in the horizontal plane.

Summary: Electromagnetic visualization shows many of the basic physical processes by which energy radiates, propagates, and reflects. Visualization aids in identifying scattering mechanisms. Once we are better able to understand how energy is scattered or how an antenna radiates, then we are better able to modify the scattering/radiating structure for more desirable results.

References

1. John Shaeffer, Kam Hom, Craig Baucke, Brett Cooper, and Noel Talcott, Jr., “Bistatic k-Space Imaging for Electromagnetic Prediction Codes for Scattering and Antennas”, NASA Technical Paper 3569, July 1996
2. John Shaeffer, Kam Hom, Craig Baucke, Brett Cooper, and Noel Talcott, Jr., “A Review of Bistatic k-Space Imaging for Electromagnetic Prediction Codes for Scattering and Antennas”, IEEE Antennas and Propagation Magazine, Feature Article, vol. 39, no. 5, October, 1997.
3. Kam Hom, Noel Talcott, Jr., and John Shaeffer, “Computational Diagnostic Techniques for Electromagnetic Scattering: Analytical Imaging, Near Fields, and Surface Currents”, ACES, March 17-21, 1997.
4. John Shaeffer, “MOM3D Method of Moments Code Theory Manual”, NASA CR 189594, Contract NAS1-18603, March 1992.
5. Kam Hom, “EM Animate: A Computer Program for Displaying and Animating Electromagnetic Near Field and Surface-Current Solutions”, NASA Technical Memorandum 4539, May 1994.
6. Helen Wang; Michael Sanders; Alex Woo: “Radar Cross Section Measurement Data of the VFY218 Configuration”, NAWC WPNS TM 7621, January 1994.

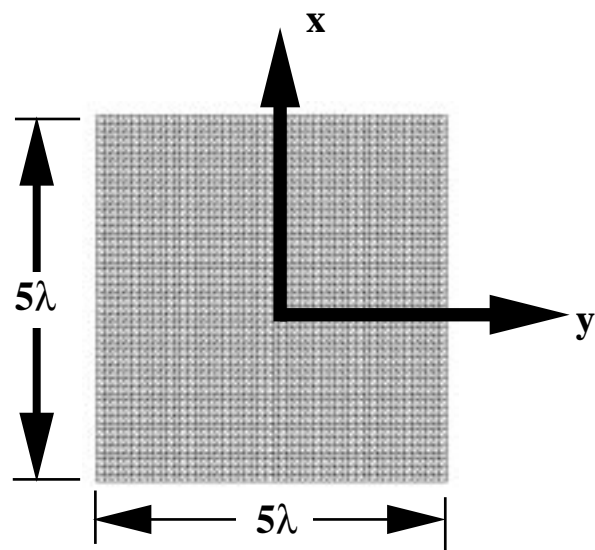
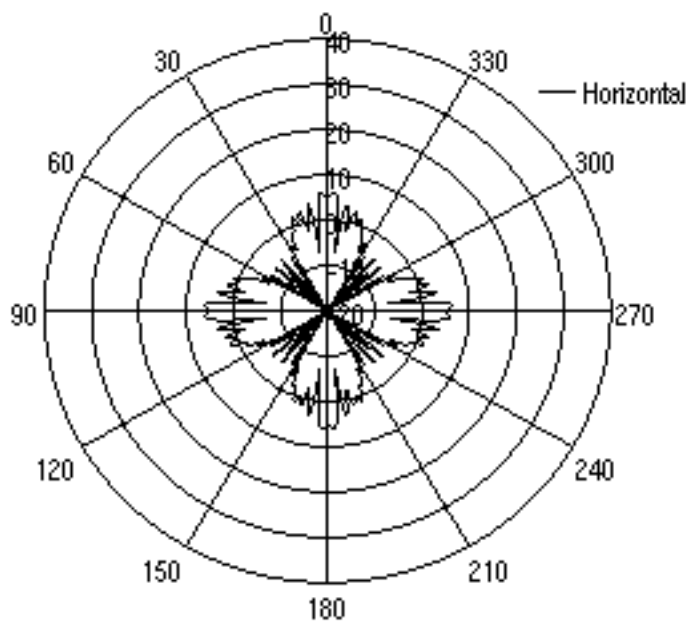
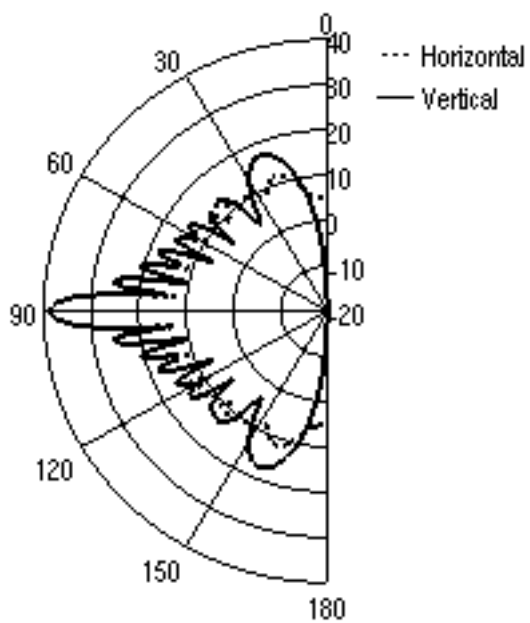


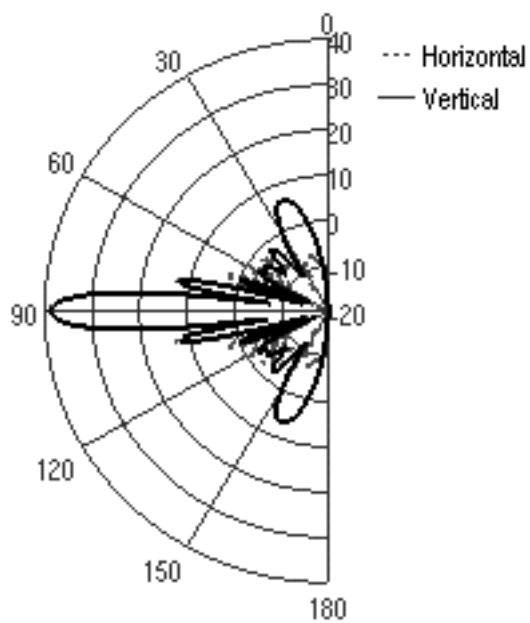
Figure 1. – Plate geometry and coordinate system.



c) Azimuth cut, el = 0. deg.



a) Elevation cut, az = 0. deg.

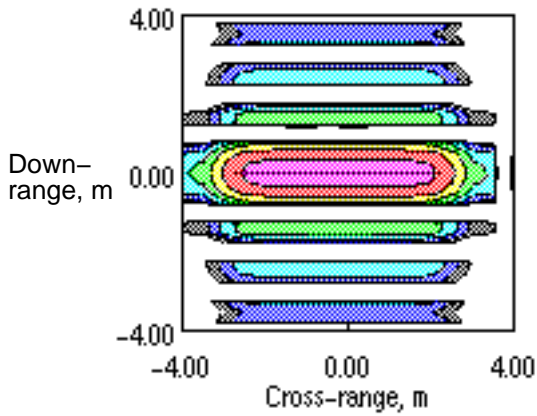


b) Elevation cut, az = 45. deg.

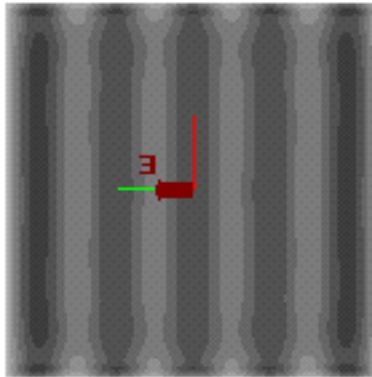
Figure 2. – Backscatter RCS patterns at different plane cuts.

Min. Contour = -40 dB,
10 dB increments.

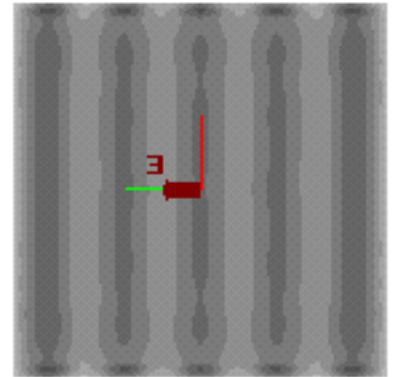
Image



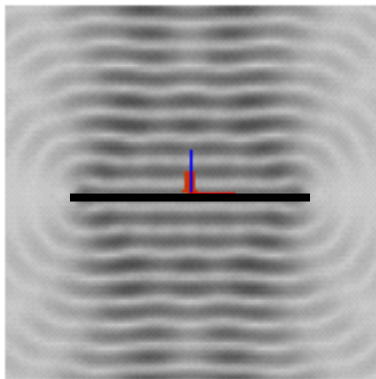
$t = 0.$



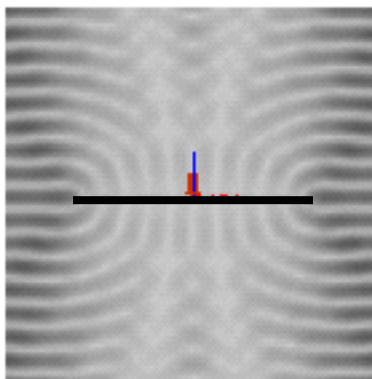
RMS



$t = 0.,$ Scattered Field



Max. Field Value = 2 V/m
 $t = 0.,$ Total Field



RMS, Total Field

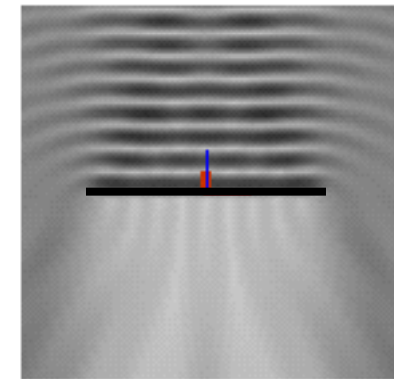
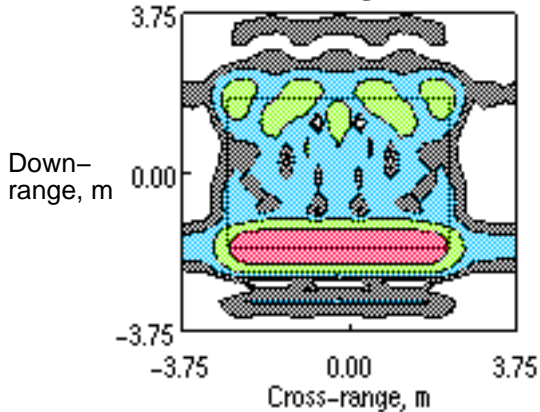
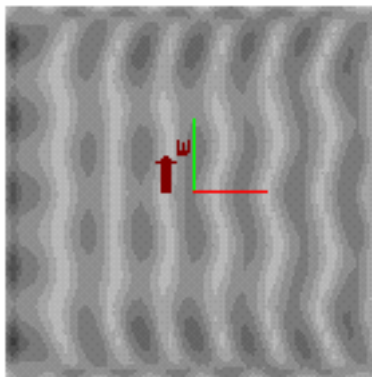


Figure 3. – Currents, radiation image, and fields: perpendicular to plate, E phi polarization.

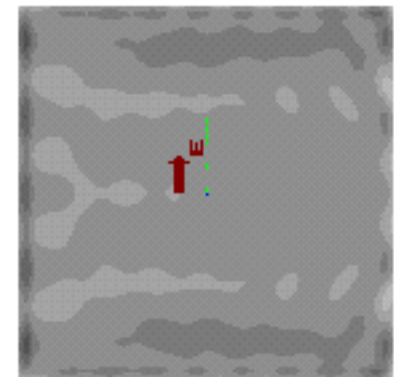
Image



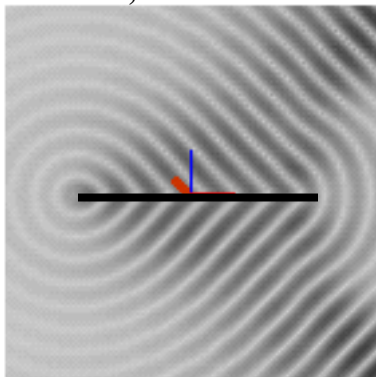
$t = 0.$



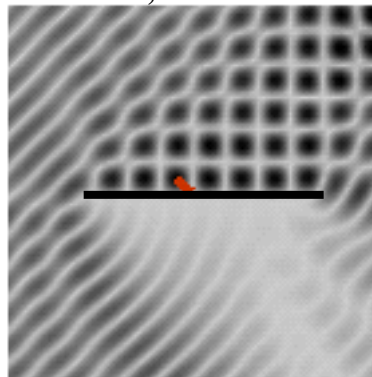
RMS



$t = 0.,$ Scattered Field



Max. Field Value = 2 V/m
 $t = 0.,$ Total Field



RMS, Total Field

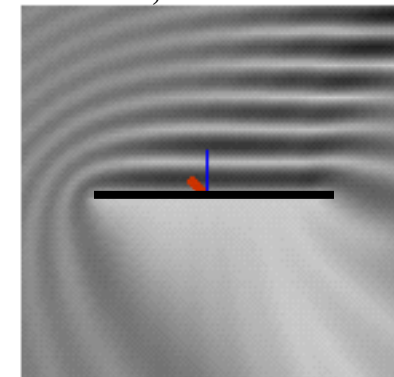


Figure 4. – Currents, radiation image, and fields: 45° specular to plate, E phi polarization.

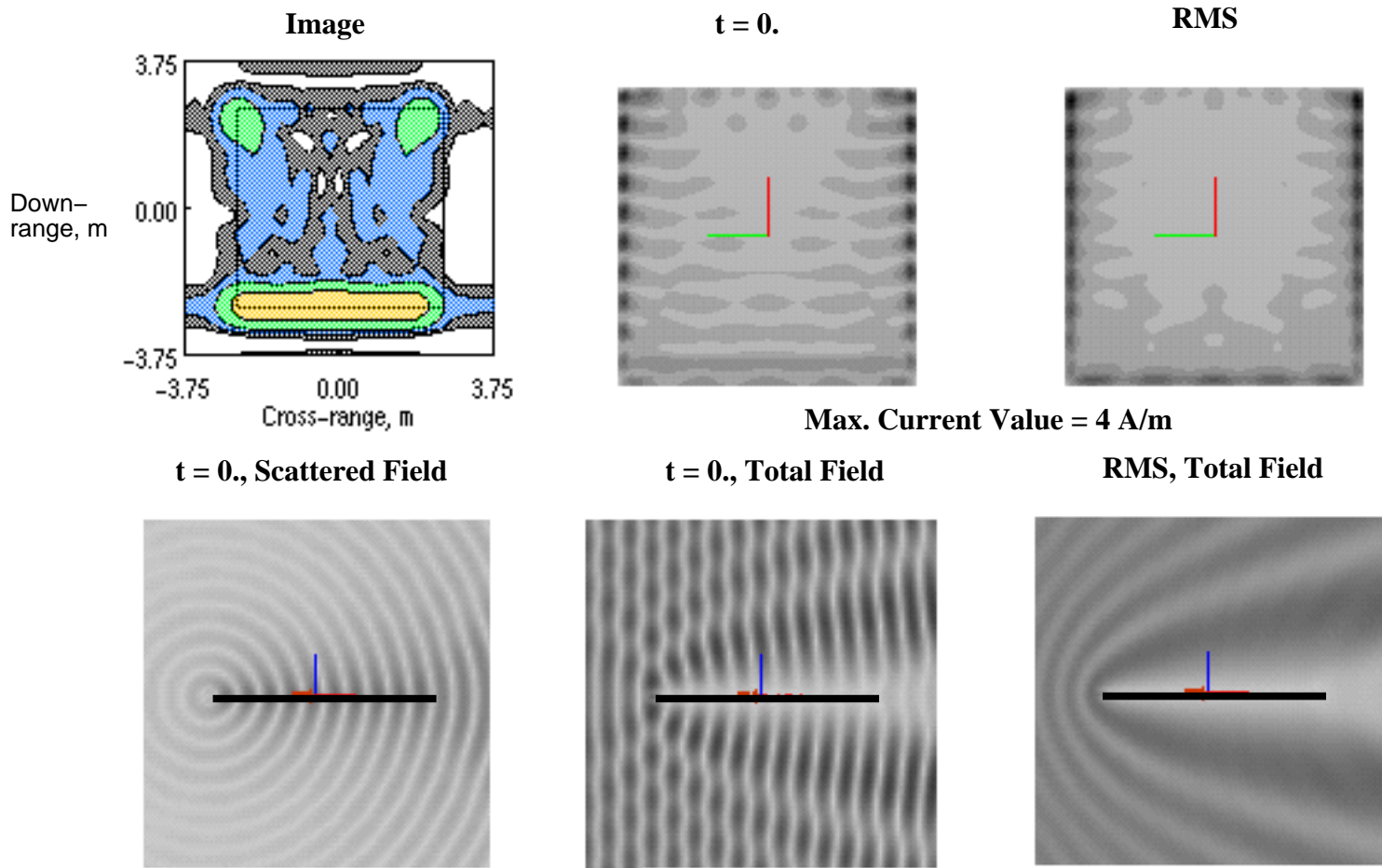


Figure 5. – Currents, radiation image, and fields: 0° azimuth, 0° elevation, E phi polariztion.

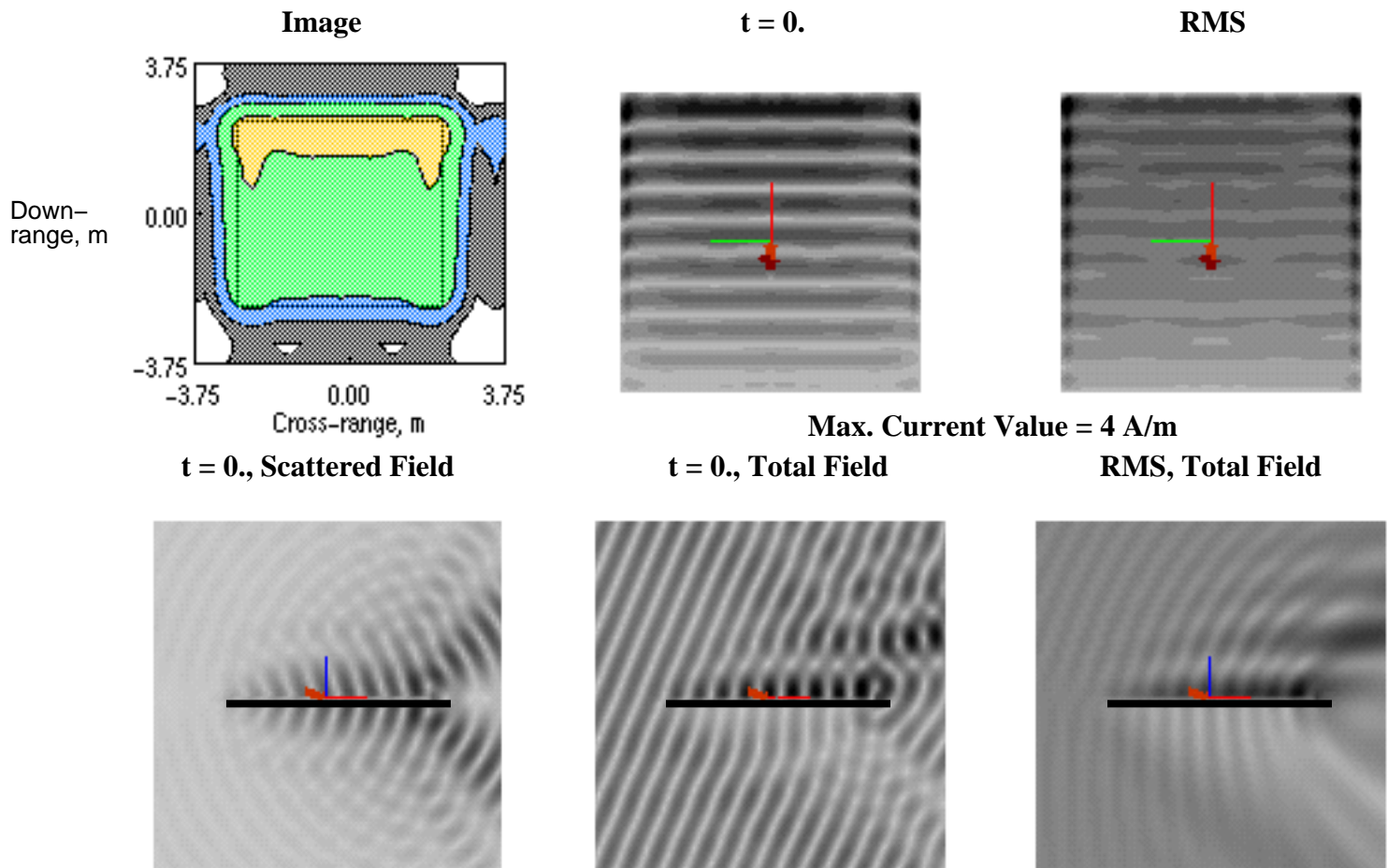
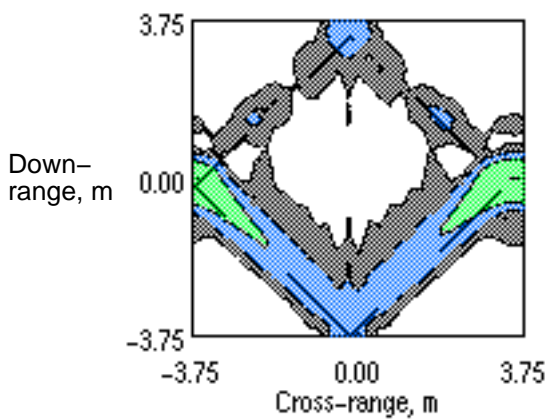
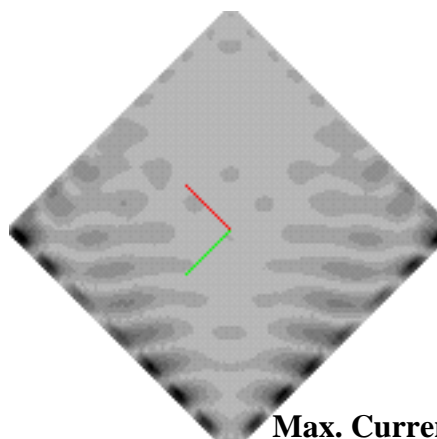
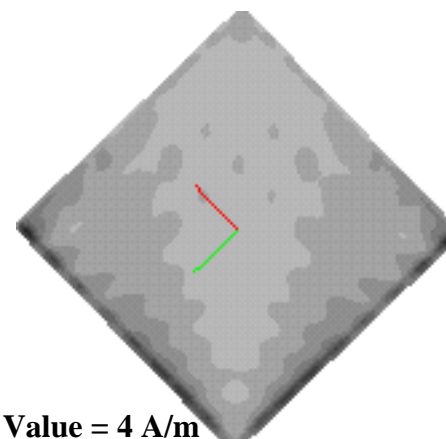
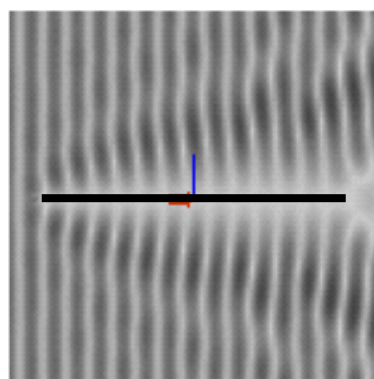
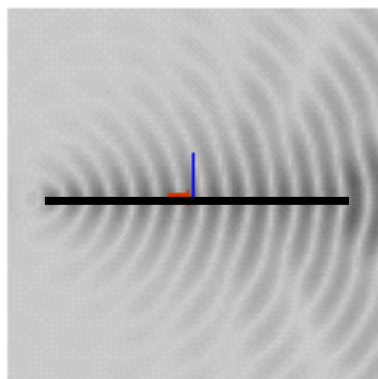


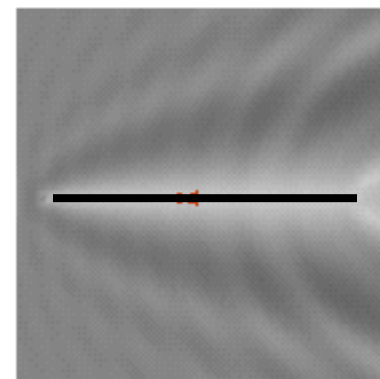
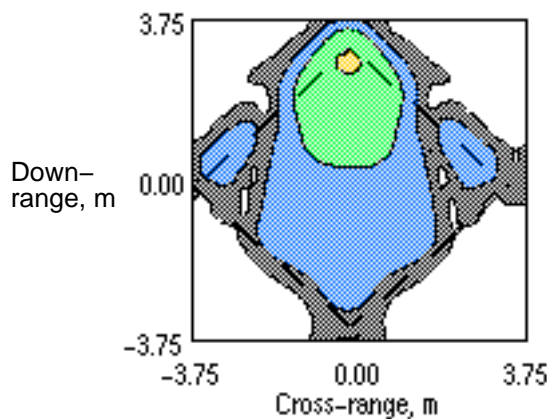
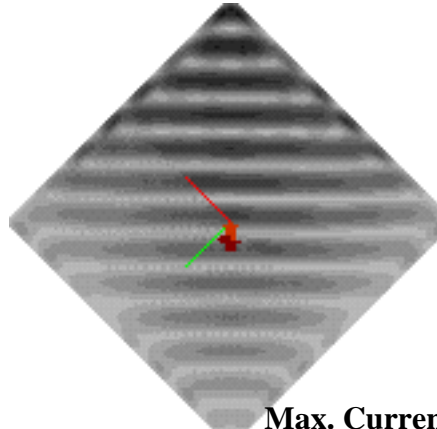
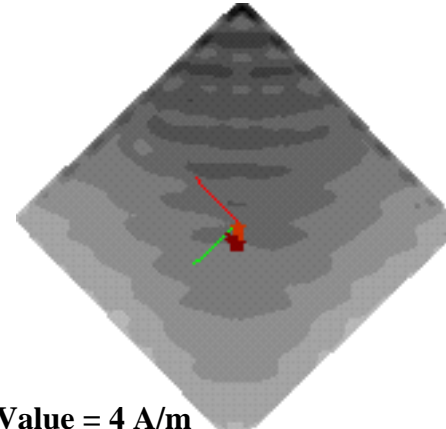
Figure 6. – Currents, radiation image, and fields: 0° azimuth, 22.5° elevation, E theta polariztion.

Image $t = 0.$, Scattered Field **$t = 0.$**  $t = 0.$, Total Field**RMS**

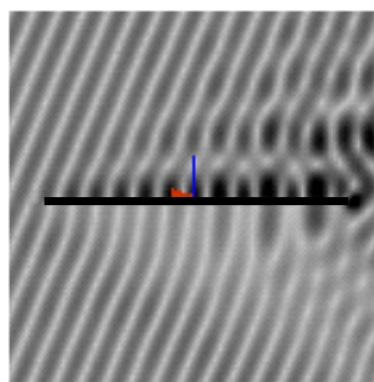
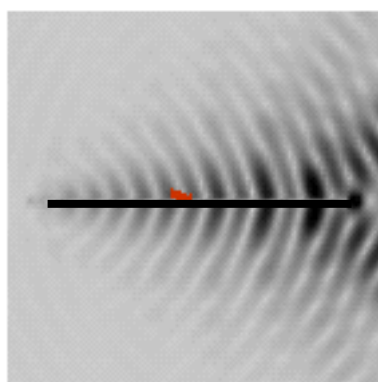
RMS, Total Field



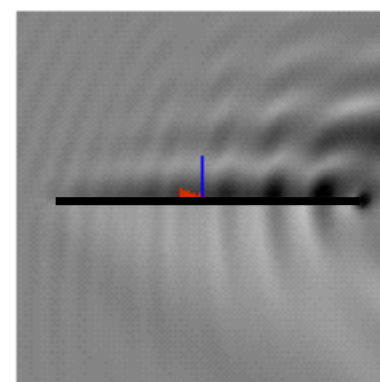
Max. Field Value = 2 V/m

**Figure 7. – Currents, radiation image, and fields: 45° azimuth, 0° elevation, E phi polariztion.****Image** $t = 0.$, Scattered Field **$t = 0.$**  $t = 0.$, Total Field**RMS**

RMS, Total Field



Max. Field Value = 2 V/m

**Figure 8. – Currents, radiation image, and fields: 45° azimuth, 22.5° elevation, E theta polariztion.**

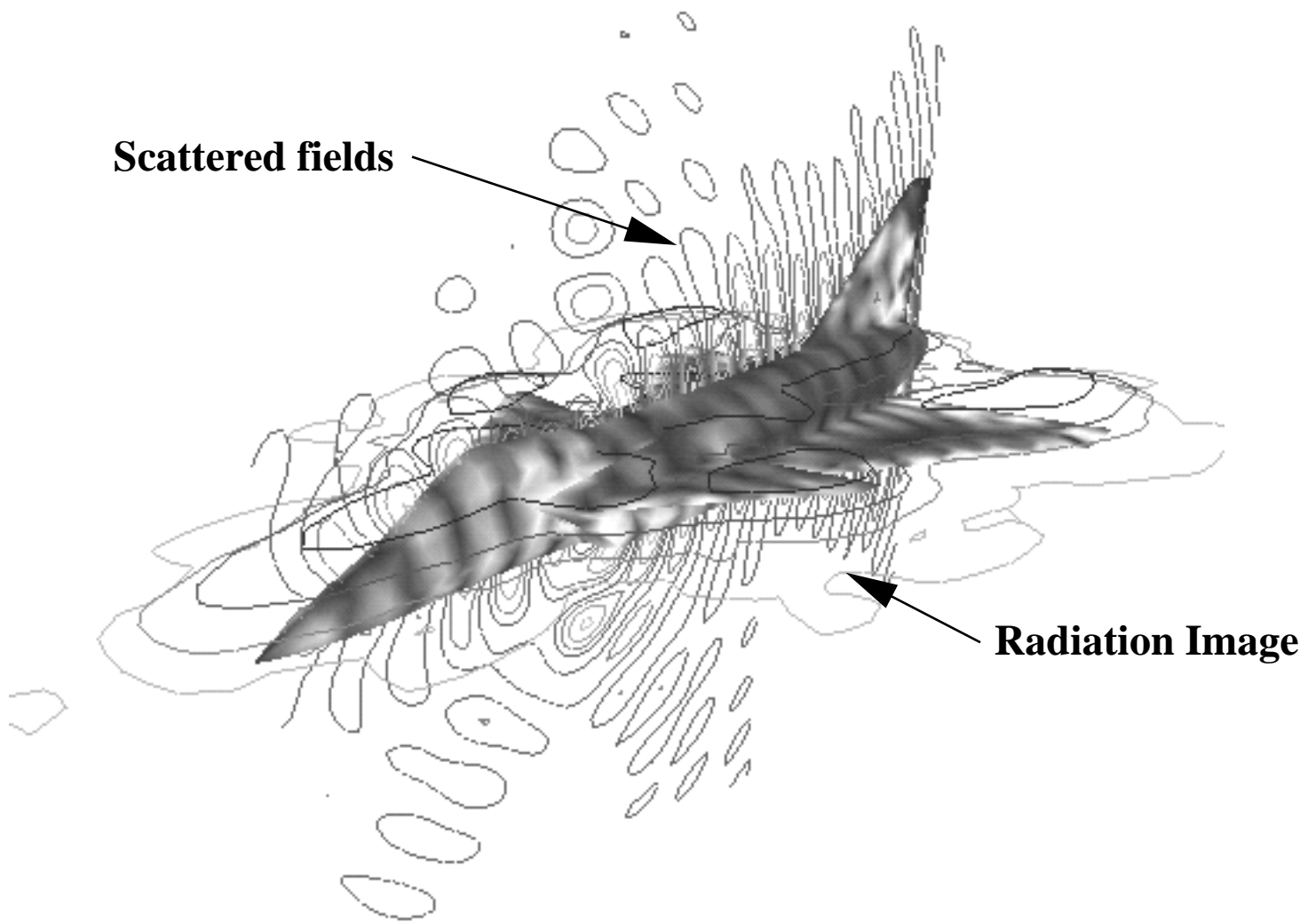


Figure 9. – Currents, radiation image, and scattered fields for VFY218, 0° azimuth, 0° elevation, E phi polariztion.